Centrifuge Modelling of Marginal Soil Slopes Under Rainfall with Hybrid Geosynthetic Inclusions

Dipankana Bhattacherjee and B. V. S. Viswanadham

Abstract The present study focuses on investigating the effect of inclusion of an innovative hybrid geosynthetic on the seepage, deformation and stability aspects of marginal soil slopes subjected to rainfall. Model hybrid geosynthetics were prepared in the study by integrating the drainage potential of nonwoven geotextile with the reinforcement function of woven geogrid. The model soil was a blend of fine sand and kaolin in the ratio of 4:1 by dry weight. The silty sand exhibited a percentage of fines equal to 20% and a saturated permeability of 1.54×10^{-6} m/s, thereby representing the properties of marginal soils found in major portions of India and other parts of the world. Centrifuge-based physical modelling was adopted at 30 gravities on slopes of 7.2 m height and crest width of 7.5 m using the 4.5 m radius beam centrifuge facility available at IIT Bombay, India. Rainfall was simulated using a custom-designed rainfall simulating assembly for a prototype rainfall intensity of 20 mm/h. It was observed that the unreinforced slope model experienced a catastrophic failure, while the hybrid geosynthetic reinforced slope experienced negligible deformation throughout the rainfall event. The surface settlements and slope face movements decreased substantially by about 94% and 71%, respectively, owing to the geogrid component. Further, the inclusion of geotextile component of hybrid geosynthetics resulted in a reduction of pore water pressures by almost 66%, thereby indicating the importance of hybrid geosynthetics in alleviating the instability of marginal soil slopes subjected to rainfall. Use of hybrid geosynthetics thus facilitate the use of marginal soils in reinforced earth construction, thereby economizing the project.

Keywords Slope stability · Hybrid geosynthetics · Rainfall · Centrifuge test · Marginal soils

D. Bhattacherjee (✉)
Department of Civil Engineering, Indian Institute of Engineering Science and Technology, Shibpur, Howrah 711103, India
e-mail: dipankana@civil.iiests.ac.in; dipankanabhattacherjee@gmail.com

B. V. S. Viswanadham
Department of Civil Engineering, Indian Institute of Technology Bombay, Powai, Mumbai 400076, India
e-mail: viswam@civil.iitb.ac.in

T. G. Sitharam et al. (eds.), *Ground Improvement Techniques*, Lecture Notes in Civil Engineering 118, https://doi.org/10.1007/978-981-15-9988-0_30

1 Introduction

In recent times, global warming and associated climatic changes have adversely affected the environmental balance and triggered the frequency of hydro-meteorological events. As a consequence, instability of natural and engineered soil slopes and retaining walls induced by rainfall have come to the forefront, resulting in significant economic damage and loss of life. The annual statistical review report of the Centre for Research on the Epidemiology of Disasters [1] reveals that, in the year 2016, almost 75% of the natural disasters that occurred in the country may be attributed to rainfall, and the estimated average losses due to rainfall-triggered landslides (especially in the Himalayan regions) exceed Rs. 550 crores/year (about 77 Million US $ per year), as reported by Dahal and Hasegawa (2008) [2]. The instability may be associated primarily with the loss of soil matric suction under rainfall, leading to the build-up of positive pore water pressure within slopes. The situation aggravates if the soil used in reinforced earth construction exhibits low permeability, and cannot dissipate the pore water pressures generated during meteorological events. However, due to increasing scarcity of good quality permeable granular soil, on-site low-permeable soils (or marginal soils) are being widely utilized in the field in recent times. This has led to increased incidents of reinforced slope/wall failures, and landslides being reported owing to the reduced strength, considerable fines content, and low permeability associated with such marginal soils. An alternative mitigation methodology is to ensure freely draining condition within marginal soil slopes during rainwater infiltration for enhanced stability.

The present study focuses on investigating the effect of inclusion of a special variety of geosynthetic material, referred to as hybrid geosynthetic (or geogrid based geocomposite) on the seepage, deformation, and stability aspects of marginal soil slopes subjected to rainfall. Hybrid geosynthetic is an assembled material possessing both in-plane drainage and reinforcement characteristics derived from a nonwoven geotextile and geogrid, respectively, as investigated by Bhattacherjee and Viswanadham (2016) [3] and Viswanadham and Bhattacherjee (2015) [4]. In the literature, the use of permeable inclusions within natural and engineered slopes have been investigated by numerous researchers including Tatsuoka and Yamauchi (1986) [5], Zornberg et al. (1998) [6], Akay et al. (2014) [7], Thuo et al. (2015) [8] and Cotecchia et al. (2016) [9], whereas the importance of reinforcement function was reported by Iryo and Rowe (2005) [10], Wu and Chou (2013) [11] and Abd and Utili (2017) [12]. However, till date, studies on the potential coupling of reinforcement and drainage functions are limited, especially with respect to slope stability under rainfall condition tested in a geotechnical centrifuge. Hence, this forms a topic of major research interest. An innovative rainfall simulator was designed for inducing rainfall at high gravities, which is a novel aspect of the present research.

2 Model Materials and Scale Factors

The model soil used in slope preparation was formulated in the laboratory by blending locally available fine sand and commercially available kaolin in the ratio of 4:1 by dry weight. The model silty sand was formulated such that it has a percentage of fines equal to 20% and a saturated permeability (k_{sat}) of 1.54 × 10^{-6} m/s, thereby representing the properties of locally available marginal soils. In this regard, it should be mentioned that marginal soils are defined as that containing fines in excess of 15%, as per Christopher and Stuglis (2005) [13], and having a saturated coefficient of permeability (k_{sat}) of the order of 1 × 10^{-6} m/sec or less, as per Holtz and Kovacs (1981) [14]. Model hybrid geosynthetics (G1N1) were prepared by integrating the drainage potential of nonwoven geotextile (N1) with the reinforcement function of woven geogrid (G1). In order to minimize particle size scale effects in a centrifuge, a ratio of $S_t/D_{50} > 10$ as suggested by Izawa and Kuwano (2010) [15] was adopted during model geogrid selection, where S_t is the spacing between transverse ribs of the reinforcement and D_{50} is the average particle size of model soil. The ultimate tensile capacity (T_{gu}) and ultimate tensile strain (ε_{gu}) of model hybrid geosynthetic was evaluated as 2.1 kN/m and 22.8%, respectively, along the machine direction as per wide-width tensile test procedure outlined in ASTM D 4595 (2005) [16]. Further, the drainage potential of hybrid geosynthetic was ascertained based on the radial flow principle outlined in ASTM D 6574 (2006) [17], and a transmissivity of 1.9 × 10^{-6} m^2/s was determined in the laboratory.

Centrifuge-based physical modelling technique was adopted in the present study to replicate similar stress history and retain identical state of stresses in the model as that of the full-scale prototype. During geotechnical centrifuge testing, a centrifugal acceleration of high gravities (Ng) is applied relative to that of earth's normal gravity (g). Standard scaling relationships are employed to link the model behaviour with the corresponding prototype. The parent geotextile was scaled based on identical transmissivity requirements outlined in Raisinghani and Viswanadham (2011) [18], whereas the parent geogrid was modelled based on scaling considerations proposed by Viswanadham and König (2004) [19]. Modelling of rainfall at high gravities was performed based on standard scaling laws outlined in Tamate et al. (2010) [20] and Bhattacherjee and Viswanadham (2018a) [21].

3 Model Preparation and Test Procedure

Centrifuge-based physical modelling was performed at 30 gravities on a representative silty sand slope of 240 mm height, 60 mm base layer and 2 V:1H inclination, having a crest width of 250 mm. Tests were conducted using the 4.5 m radius beam centrifuge facility available at IIT Bombay, INDIA. The above gravity level (30 g) and radius of centrifuge ensured minimum scale effects due to variation of gravity level with model depth and horizontal distance in the model, as outlined in Taylor (1995)

[22]. The model slope corresponded to a prototype height of 7.2 m and a crest width of 7.5 m in the field. Rainfall was simulated using a custom-designed rainfall simulating assembly consisting of spray nozzles, nozzle hanging rods, nozzle assembly attaching plate, a water container assembly with support system and additional components involving a solenoid valve, a seepage tank and run-off collector. Adequate measures were taken to minimize the effects of Coriolis force generated at high gravities by enabling a shift in the position of nozzles depending upon the direction of centrifugal rotation. The nozzles are specially designed pneumatic nozzles capable of producing fine mist at a uniform rate in-flight condition for intensities ranging from 2 mm/h to as high as 80 mm/h. A set of four nozzles were placed at the slope crest, while another four were placed at the inclined face to ensure uniform distribution of rainfall over the slope surface. The slopes were instrumented with four pore pressure transducers (PPTs) placed above the base layer at distances of 20 mm (PPT4), 125 mm (PPT3), 250 mm (PPT2), and 350 mm (PPT1) from the perforated face of the seepage tank in model dimensions. Further, L-shaped plastic markers made from thin transparency sheets of 20 mm × 10 mm dimensions were embedded within the slope front elevation to track slope displacements with the progress of rainfall. Additional L-shaped plastic markers were glued on to the slope face to facilitate computation of slope face movements with rainfall. The model hybrid geosynthetic (G1N1) was cut to a total length of ($L_A + L_F + L_R$) and to a width of 200 mm. The anchorage length (L_A) was equivalent to 0.25 times the model slope height h, L_F represented the length along the slope face and the reinforcement length (L_R) was 0.85 h. The various stages involved in the construction of unreinforced and reinforced slope models in the centrifuge are discussed elaborately in Bhattacherjee and Viswanadham (2018b) [23]. The response of unreinforced and reinforced slope models was monitored for a prototype rainfall intensity of 20 mm/h, which corresponds to a heavy rainfall event as per standard global thresholds of Llasat (2001) [24].

4 Results and Discussion

The surface settlements, slope face movements, and pore water pressure profiles developed during rainfall at various time intervals were investigated in the present study based on data recorded by pore water pressure transducers and through image analysis [25] of selected images captured during centrifuge tests. The results of two centrifuge model tests (T1 and T2) are discussed in this section, wherein Model T1 represents an unreinforced slope and Model T2 corresponds to a reinforced slope with six layers of hybrid geosynthetic (G1N1) inclusions. In both the cases, an initial water table was maintained up to the slope toe at the onset of rainfall by means of horizontal seepage induced by a seepage tank. The duration of centrifuge tests was maintained as 30 min (18.75 days in prototype dimensions) from the period of starting rainfall for the reinforced slope (Model T2), or until failure in case of the unreinforced slope (Model T1).

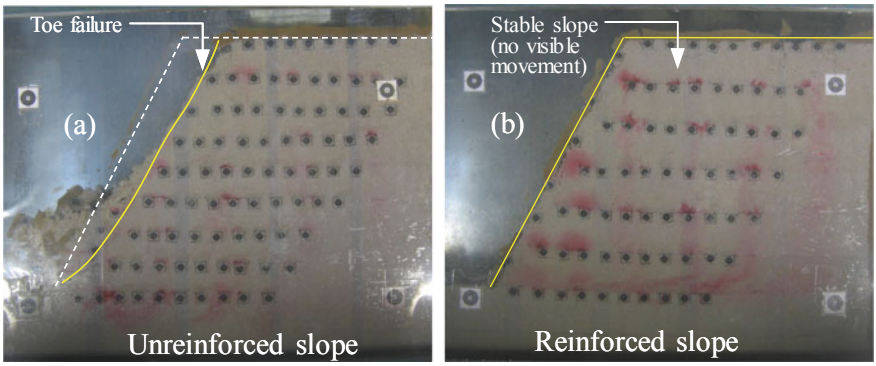

Fig. 1 Front elevation of slopes **a** Model T1 [$t = 9.375$ days] **b** Model T2 [$t = 18.75$ days]

4.1 Deformed Slope Profiles Observed Post Rainfall

The front elevation of unreinforced and hybrid geosynthetic reinforced slopes captured during the ultimate stage of centrifuge tests at the end of 9.375 days and 18.75 days of rainfall (in prototype dimensions) are presented in Fig. 1a, b respectively. It can be observed from Fig. 1a that the unreinforced slope (Model T1) experienced a catastrophic toe failure due to rainwater infiltration. However, the hybrid geosynthetic reinforced slope (Model T2) was stable throughout the rainfall event, with no visible slope movements captured until the end of the rainfall event shown in Fig. 1b.

4.2 Pore Water Pressure Generation with Rainfall

The pore water pressure generation during rainfall for unreinforced slope and hybrid geosynthetic reinforced slope are shown in Fig. 2. The values measured by PPT3 ($u_{PPT3}/\gamma h$) placed vertically below the mid-point of the crest of the slope on the base layer are herein presented. The pore pressures (u) are normalized with respect to the unit weight of model soil (γ) multiplied by the slope height (h), and are expressed in prototype dimensions, starting from the time of occurrence of rainfall. As visible from Fig. 2, the unreinforced slope Model T1 exhibited increasing $u_{PPT3}/\gamma h$ values with rainfall, the peak value being 0.438. On the contrary, the slope model reinforced with hybrid geosynthetic layers, namely Model T2 (G1N1) exhibited lower $u_{PPT3}/\gamma h$ values for the entire duration of tests with a peak value of 0.028. The maximum normalized pore pressure ($u_{max}/\gamma h$) recorded by PPT4 for both the models are presented in Table 1, which indicates that the presence of hybrid geosynthetics resulted in a reduction of pore water pressure values by almost 66%. The above implies the effectiveness of the geotextile component of hybrid geosynthetics in

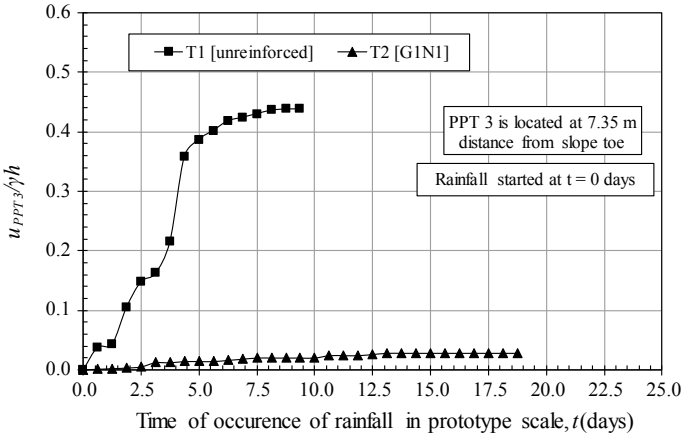

Fig. 2 Variation of normalized excess pore water pressure with rainfall

Table 1 Summary of test results

Parameter	Model T1 [Unreinforced]	Model T2 [Reinforced]
Time elapsed during rainfall (days)	[a]9.375	[b]18.75
[c]$u_{max}/\gamma h$	0.554	0.185
$S_{c,max}/h$	0.492	0.020
$S_{f,max}/h$	0.166	0.048

Note All values are reported in prototype dimensions; *h:* Height of slope; u/γh: Normalized pore water pressure; $S_{c,max}$: Max. crest settlement; $S_{f,max}$: Max. deformation along slope face; [a]Time corresponding to failure; [b]During ultimate stage of test, beyond which no significant variations in pore water pressure magnitudes or slope deformation was observed; [c]For PPT4 placed at 350 mm from slope toe

dissipating the excess pore water pressures generated during a rainfall event, thereby ensuring the stability of the slope under rainfall conditions.

4.3 Variation of Surface Settlements with Rainfall

Figure 3 presents the variation of surface settlements measured from the slope crest at the ultimate stage of the tests. As evident from Fig. 3, the unreinforced slope (Model T1) showed a gradual increase in surface settlement with rainfall of 20 mm/h, the maximum value being 3.54 m (in prototype dimensions) at the crest at the ultimate

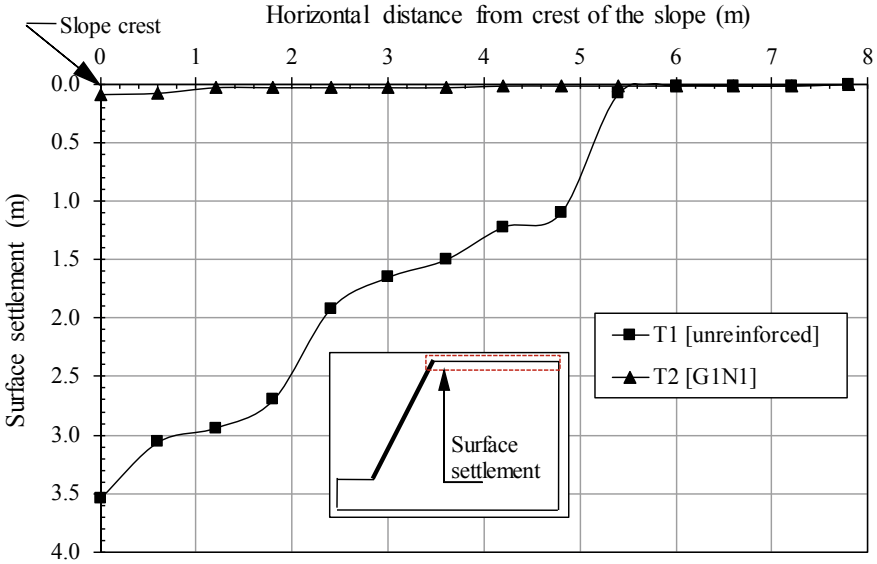

Fig. 3 Variation of surface settlements from slope crest with rainfall

stage. This high magnitude of deformation is attributed to the absence of reinforcement function within the marginal soil slope subjected to rainfall. On the contrary, the slope reinforced with hybrid geosynthetic layers (Model T2) recorded negligible settlement of the order of 0.092 m (in prototype dimensions) under the same rainfall intensity of 20 mm/h, as can be seen from Fig. 3. Hence, the inclusion of hybrid geosynthetics resulted in reduced vertical settlements at slope surface by about 94%.

4.4 Slope Face Movements with Rainfall

Figure 4 presents the displacements observed at the slope face with the progress of rainfall, obtained by tracking the co-ordinates of inclined markers at the slope face in case of unreinforced slope (Model T1), and that of plastic markers stuck to hybrid geosynthetic layers facing towards the slope face for reinforced slope (Model T2). The face movements have been plotted considering the slope face to be vertical, and coinciding with the vertical axis and origin at the toe. As evident from Fig. 4, the unreinforced slope (Model T1) recorded a sudden displacement at the toe in the order of about 1.20 m in prototype dimensions at the time of failure ($t = 9.375$ days). This may be attributed to the building up of pore water pressures within the slope due to rainfall [observed previously in Fig. 2], giving rise to positive seepage forces.

On the contrary, the slope reinforced with hybrid geosynthetic layers (Model T2) depicted a negligible increase in lateral displacements at slope face with rainfall,

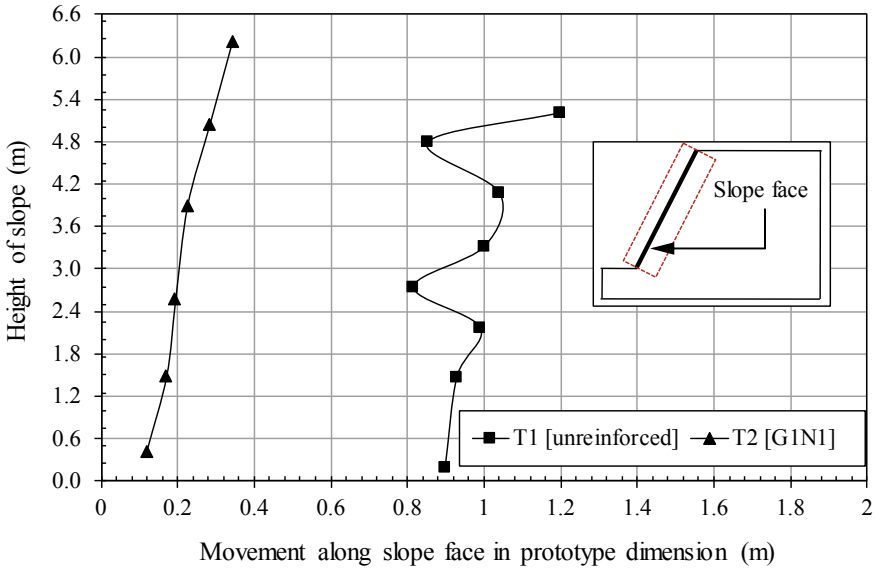

Fig. 4 Slope face movements observed during rainfall

the maximum value being 0.36 m in prototype scale ($t = 18.75$ days). Hence, the geogrid component of hybrid geosynthetics resulted in reduced slope face movements by about 71% as compared to unreinforced marginal soil slopes. The results derived from the centrifuge model tests conducted in the present study are hereby summarized in Table 1.

5 Conclusions

The present study highlights the importance of coupling the two functions of drainage and reinforcement offered by geogrid and nonwoven geotextile, respectively, into one integral material referred to as hybrid geosynthetic for improving the performance of marginal soil slopes subjected to rainfall. Modelling of hybrid geosynthetics in a geotechnical centrifuge and use of the same in alleviating the problems associated with marginal soil slopes under rainfall using an innovative in-flight rainfall simulator developed for this purpose may be considered as the novel aspects of the present study. Based on the centrifuge model tests conducted in the study, it is inferred that the unreinforced slope model experienced a catastrophic failure and increasing phreatic levels with rainfall. On the contrary, the hybrid geosynthetic reinforced slope experienced negligible deformation throughout the rainfall event, and the surface settlements and slope face movements decreased substantially by about

94% and 71%, respectively, owing to the geogrid component. Further, the inclusion of geotextile component of hybrid geosynthetics resulted in a reduction of pore water pressure values by almost 66%. The above finding facilitates the use of soils available locally at the construction site in infrastructural projects, thereby economizing project costs, and preventing to a large extent the unsustainable over-mining of natural sand deposits for construction purposes.

References

1. CRED (Centre for Research on the Epidemiology of Disaster) (2012) Annual Disaster Statistical Review 2011: The Numbers and Trends. Research Unit, Université Catholique de Louvain, Louvain-la-Neuve, Belgium, CRED
2. Dahal RK, Hasegawa S (2008) Representative rainfall thresholds for landslides in the Nepal Himalaya. Geomorphology 100(3–4):429–443
3. Bhattacherjee D, Viswanadham BVS (2016) Effect of hybrid geosynthetic layers on soil walls with marginal backfill subjected to rainfall. In: De A, Reddy KR, Yesiller N, Zekkos D, Farid A (eds.) Proceedings of Geo-Chicago 2016, Geotechnical Special Publication No 269, ASCE (Pubs.), pp 362–371
4. Viswanadham BVS, Bhattacherjee D (2015) Studies on the performance of Geocomposite reinforced low-permeable slopes subjected to rainfall. Japn Geotech Soc Spe Pub 2(69):2362–2367
5. Tatsuoka F, Yamauchi H (1986) A Reinforcing Method for Steep Clay Slopes using Non-woven Geotextile. Geotext Geomembr 4(3–4):241–268
6. Zornberg JG, Sitar N, Mitchell JK (1998) Performance of geosynthetic reinforced slopes at failure. J Geotech Geoenviron Eng 124(8):670–683
7. Akay O, O¨zer AT, Fox GA, (2014) Assessment of EPS block geofoam with internal drainage for sandy slopes subjected to seepage flow. Geosyn Int 21(6):364–376
8. Thuo JN, Yang KH, Huang CC (2015) Infiltration into unsaturated reinforced slopes with nonwoven geotextile drains sandwiched in sand layers. Geosyn Int 22(6):457–474
9. Cotecchia F, Lollino P, Petti R (2016) Efficacy of drainage trenches to stabilise deep slow landslides in clay slopes. Géotechnique Let 6(1):1–6
10. Iryo T, Rowe RK (2005) Hydraulic behaviour of soil geocomposite layers in slopes. Geosyn Int 12(3):145–155
11. Wu JY, Chou NN (2013) Forensic studies of geosynthetic reinforced structure failures. J Perform Construct Facil ASCE 27(5):604–613
12. Abd AH, Utili S (2017) Design of geosynthetic-reinforced slopes in cohesive backfills. Geotext Geomembr 45(6):627–641
13. Christopher BR, Stuglis RS (2005) Low permeable backfill soils in geosynthetic reinforced soil wall: State of the practice in North America. In: Proceedings of North American Geosynthetics conference (NAGS2005), GRI-19, Las Vegas, USA, pp 14–16
14. Holtz RD, Kovacs WD (1981) An introduction to geotechnical engineering Prentice Hall. Englewood Cliffs, New Jersey
15. Izawa J, Kuwano J (2010) Centrifuge modelling of geogrid reinforced soil walls subjected to pseudo-static loading. Int J Phys Modell Geotech 10(1):1–18
16. ASTM D 4595 (2005) Standard test method for tensile properties of geotextile by the wide-width strip method, Annual Book of ASTM Standards, Section 4, Volume 04.13, Geosynthetics, American Society for Testing and Materials, West Conshohocken, Pennsylvania, USA
17. ASTM D 6574 (2006) Standard test method for determining the (in-plane) hydraulic transmissivity of a geosynthetic by radial flow, American Society for Testing and Materials, West Conshohocken, Pennsylvania, USA

18. Raisinghani DV, Viswanadham BVS (2011) Centrifuge model study on low permeable slope reinforced by hybrid geosynthetics. Geotext Geomembr 29(6):567–580
19. Viswanadham BVS, König D (2004) Studies on scaling and instrumentation of a geogrid. Geotext Geomembr 22(5):307–328
20. Tamate S, Suemasa N, Katada T (2010) Simulating shallow failure in slopes due to heavy precipitation. In: Springman S, Laue J, Seward L (eds.) Proceedings of the 7th international conference in physical modelling in geotechnics – 7th ICPMG, Switzerland Taylor and Francis group (Pubs.), vol 2, pp 1143–1149
21. Bhattacherjee D, Viswanadham BVS (2018) Design and Performance of an Inflight Rainfall Simulator in a Geotechnical Centrifuge. Geotech Test J 41(1):72–91
22. Taylor RN (1995) Centrifuges in modelling: principles and scale effects. Geotechnical Centrifuge Technology, Blackie Academic and Professional, Glasgow, U.K.
23. Bhattacherjee D, Viswanadham BVS (2018) Effect of geocomposite layers on slope stability under rainfall condition. Indian Geotech J 48(2):316–326
24. Llasat MC (2001) An objective classification of rainfall events on the basis of their convective features. Int J Climatol 21(1):1385–1400
25. Image-Pro Plus (2004) Image-Pro Plus Manual. Ver. 5.1. Media Cybernetics, Inc., USA